

Different Applications of Energy Recovery Linacs

K. Aulenbacher

Institut für Kernphysik der Johannes Gutenberg-Universität, Mainz, Germany

Abstract

Besides their application for radiation generation, energy recovery linacs may become a unique tool for scattering experiments in nuclear and particle physics. Applications for fixed target and also for collider experiments are discussed. Spin polarized operation is an essential feature which requires additional attention.

Keywords

Energy recovery linac; electron ion collider; Mainz energy-recovering superconducting accelerator.

1 Introduction

The proposal to use energy recovery for electron-collider experiments by Maury Tigner dates back to the 1960s [1]. However, it soon became apparent that synchrotrons would offer better conditions, thus the idea was not pursued intensely until the end of the century. Nowadays, the limitations of the storage ring concept are well known and scientists have revisited the advantages linac-based experiments would offer. The advantages of Energy Recovery Linacs (ERLs) for radiation production have been discussed in another contribution to this school [2]. In this paper I will mention the possibilities for scattering experiments with ERLs that serve particle or nuclear physics studies.

Such experiments have been pursued in the past with linacs and also storage rings, the Stanford Linear Collider (SLC) and the Large Electron Positron collider (LEP) being typical large-scale examples. In Section 2 I will address the specific advantages that ERLs may offer compared to the established systems. Typical experiments are discussed together with their physics goals in Section 3. Present ERL designs always incorporate recirculations, therefore their energy range is limited to ≈ 100 GeV due to synchrotron radiation losses. In this energy region, the investigation of spin-dependent interactions is an important possibility. The requirements of spin operation are discussed in the final Section 4, together with some specific hardware needed for such experiments.

2 Applications for ERLs in particle physics

ERLs have hitherto not been used for particle physics experiments, although the initial suggestion of Tigner pointed in exactly this direction. The reason is of course that other accelerator types have served the purposes of particle physics with extraordinary success. However, accelerator-based experiments are presently facing tremendous challenges. One of these challenges, increasing the beam energy, cannot be efficiently addressed with present-day electron ERLs due to the fact that the recirculation system will produce intense synchrotron radiation and consequently limit the luminosity at high energies. The advantages of ERLs have therefore to be sought at low energies (<100 GeV or even much lower) where unprecedented experimental conditions can be achieved which are not accessible with the established accelerators. Two such regimes have been proposed, which we discuss in the following subsections.

2.1 Low background in fixed target experiments at low energies

If a beam hits a target at rest which has dimensions larger than the beam itself, the reaction rate is given by

$$R = L \cdot \frac{d\sigma}{d\Omega} \Delta\Omega \quad (1)$$

The symbols denote L : luminosity, $\frac{d\sigma}{d\Omega}$ differential cross-section, $\Delta\Omega$: solid angle of the detector system. If the interest of the experimenter is in achieving high statistical accuracy—for instance if the cross-section to be measured is very low—a high luminosity is desired. In a fixed target experiment the luminosity can be increased by a high areal density which represents the product of the density ρ and the thickness (d_{target}) of the target:

$$L = \frac{N_A}{A} \frac{I_{\text{beam}}}{e} \rho_{\text{Target}} d_{\text{target}} \quad (2)$$

where e = electron charge, N_A = Avogadro's number, and A = atomic mass unit of the target.

Conventional fixed target experiments have the advantage of a potentially very high luminosity, for instance, the planned P2 experiment at the Mainz Energy-recovering Accelerator (MESA) facility in Mainz will be operated with a 60 cm long liquid hydrogen target and an external beam current (without energy recovery) of 150 μA [3], yielding a luminosity of $>10^{39} \text{ cm}^{-2} \text{ s}^{-1}$. In this experiment, the areal density of the scattering centres which contribute to the reactions is approximately $2.5 \times 10^{24} \text{ cm}^{-2}$.

The large number of scattering centres in the target creates limitations for precision experiments in several ways. One of them is the uncertainty caused by multiple scattering in the target which sets limits to the precision of the determination of scattering angle, energy loss, etc. Furthermore, multiple scattering leads to tails in the angular distribution which can cover large angular intervals. In consequence, the background created from such halo particles when they hit structural components in the vicinity of the experiment creates another source of systematic uncertainty. Yet another contribution of this kind is the enclosure of the target, which represents another background source. Moreover, the scattered signal particles have to penetrate the enclosure too. This will straggle their angular and energy distribution and hence further reduce the measurement accuracy. These effects become more and more pronounced with decreasing energy.

Whereas these effects are not limiting for experiments such as P2, other high-precision experiments call for a target without enclosure and low areal density. These demands are met, for instance, by gas jets—such targets are also called ‘windowless gas targets’. The application of such a target, together with an ERL, was proposed by Heinemeyer et al. [4]. They observed that a thin target would only lead to a small deterioration of the beam quality which could allow for energy recovery of the beam. Figure 1 shows the schematic setup of an ERL employing such a target.

Experiments of this type have already been performed at storage rings for a long time, for instance with the HERMES target at HERA [5]. In a storage ring, precision experiments are burdened by the fact that the luminosity is varying with time and that the injection periods interrupt the data acquisition. Again, these disadvantages become more severe the lower the energy of the operation. On the other hand, in an ERL, each beam particle passes the target only once, which leads to stationary beam conditions. In order to distinguish this from the storage ring, where beam particles may pass the target billions of times, we call the ERL target a ‘pseudo internal target’ (PIT).

Therefore, in a beam energy range $<1 \text{ GeV}$, a window of opportunity may exist in which operating an ERL can enable experiments with fixed targets which have hitherto been difficult or impossible. The existing Jefferson Laboratory ERL and the MESA facility at Mainz, which is currently under construction, both operate at energies in the 100 MeV range, where the shortened beam lifetime in a storage ring would make internal target experiments difficult. Experiments at these facilities aim to demonstrate the advantages of this new type of experimental regime. I discuss several such experiments below. A very encouraging result has already been obtained by a team formed by MIT/Bates and JLAB¹. They

¹MIT=Massachusetts Institute of Technology, Boston, USA; JLAB= Jefferson Laboratory, Newport News, USA

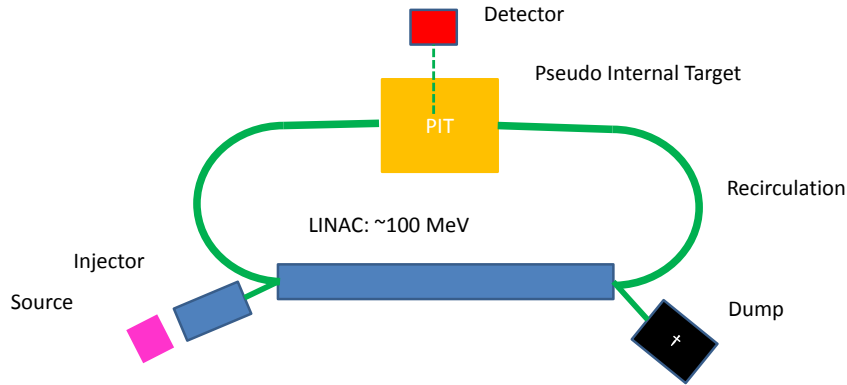


Fig. 1: Schematic of an ERL setup with ‘pseudo internal target’ (PIT)

successfully demonstrated transmission of a high intensity beam through a 127 mm long tube with a 2 mm aperture with negligible losses [6].

2.2 Electron ion colliders

Electron ion colliders (EICs) are operating in the multiple GeV energy range. They may be designed as ring/ring (RR) or as linac/ring (LR) machines. Figure 2 shows a schematic layout of such a LR configuration. Two examples which are currently under discussion for the LR configuration are the eRHIC project at BNL [7] and the LHeC [8] at CERN². In both cases, a high energy ion accelerator already exists and will be complemented by an ERL. In the BNL design, the ERL will be integrated into the already existing tunnel and at CERN a dedicated electron ring separated from the LHC tunnel will be built.

Again it is useful to discuss what the substantial advantages are that can be achieved with respect to the established RR ansatz. A first advantage is the enormously reduced complexity with respect to the spin degree of freedom. In a ring setup, depolarizing resonances have to be avoided and space consuming spin rotators are difficult to integrate. This is one of the main reasons why the LEP ring did not directly exploit spin degrees of freedom for its particle physics program, although important information was gained by using the depolarizing resonances as a tool for absolute energy calibration [9]. Such problems are virtually absent in a linac-based approach that offers high flexibility of spin orientation with very modest effort [10]. Due to the fast acceleration in the linac-type accelerator, depolarization is virtually absent.

As in the fixed target case, the luminosity is a salient ingredient to obtain sufficient reaction rates. For the case of a collider, a simplified formula under the assumption of equal emittances (ϵ) and beta functions at the interaction point (β^*) is

$$L = f_{\text{coll}} \frac{N_{\text{el}} N_{\text{Ion}}}{\epsilon \beta^*}, \quad (3)$$

where N_{Ion} is the number of ions per bunch. The bunch collision rate, f_{coll} , times the number of particles per electron bunch, $e f_{\text{coll}} N_{\text{el}}$, is the beam current which can surpass 1 A in a storage ring. The virtual

²eRHIC=electron Relativistic Heavy Ion collider at Brookhaven National Laboratory (BNL), Upton, USA, LHeC=Large electron Hadron Collider at Centre des Etudes des Recherches Nucleaires (CERN), Geneva Switzerland.

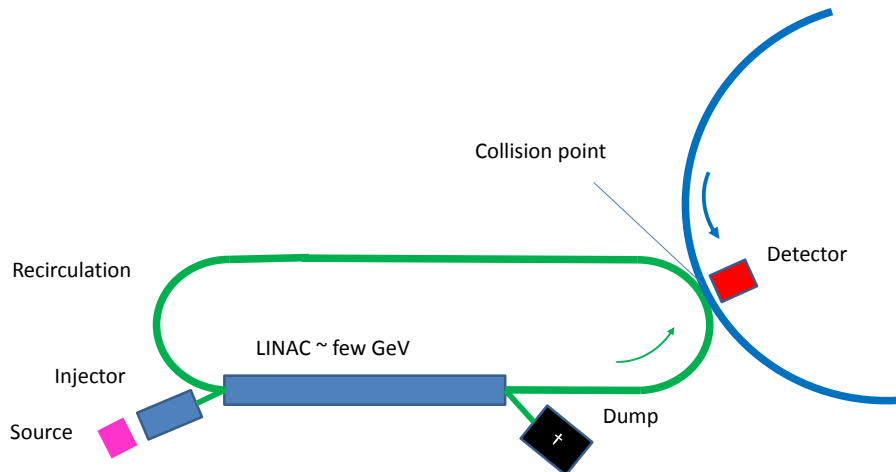


Fig. 2: Schematic layout of a linac/ring (LR) configuration

beam power at the collision point (beam current times energy) is \approx GW which is of no concern in a storage ring but makes energy recovery mandatory for a linac.

The fact that the emittance (ϵ) of the lepton beam [2] can be smaller than the equilibrium emittance in the ring can create an advantage for the generation of high luminosities. This of course also calls for a similar emittance of the ion beam. Recently, promising concepts such as coherent cooling [11] have been suggested for ion beams which might help to increase the luminosity even further. Another potential advantage can be realized if one takes into account that stable operation of a ring collider may be limited by the beam–beam tune shift which is proportional to the bunch charge of the other beam species [12].

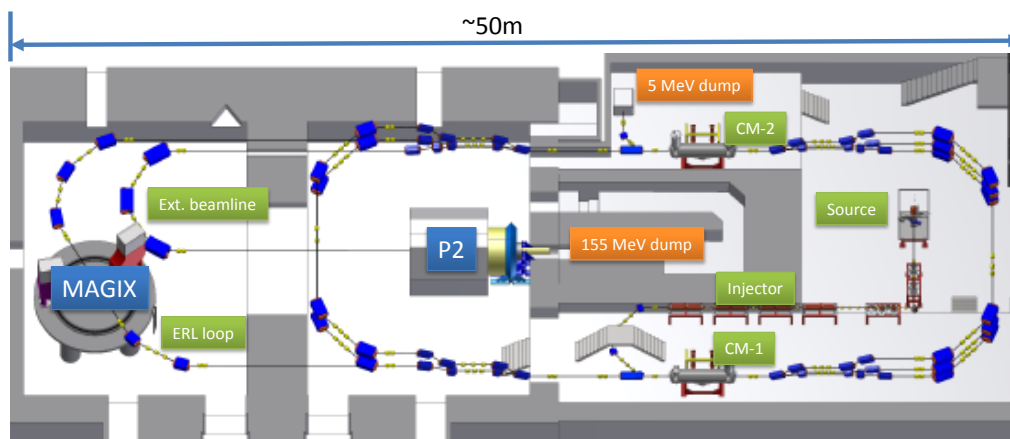
$$\Xi_{\text{Ion}} \propto \frac{N_{\text{el}}}{\gamma_{\text{Ion}}} ; \Xi_{\text{El}} \propto \frac{N_{\text{Ion}}}{\gamma_{\text{el}}}. \quad (4)$$

This offers a means to circumvent the beam tune shift by reducing the number of electrons per bunch at the expense of a higher N_{Ion} . The increased tune shift of the electrons can be handled, since the electrons pass the target only once. A further advantage is that the difficulties of producing a high average current of spin polarized electrons (see Section 4 below) can be mitigated in this regime.

It should be noted that for experiments using (polarized) *positron* beams the RR concept is better. A linac-based experiment needs a particle source with an average current in the mA range which is presently not feasible for positrons. But the majority of experiments suggested for such colliders aim at hadronic observables which are probed with the lepton beam. In this case positrons do not give much of an advantage.

3 Particle physics experiments at ERLs

As an example of possible fundamental physics applications we discuss the experimental portfolio for the MESA ERL. The ERL will be operated with a beam energy of 105 MeV. The machine is currently being built at the Johannes Gutenberg-University in Mainz, Germany. Figure 3 gives an overview of the accelerator and its experiments.



MESA accelerator at Johannes Gutenberg-Universität Mainz

Double sided recirculation design with normalconducting injector and two-sided superconducting main linac

Two different modes of operation:

- EB-operation (P2/BDX experiment): polarized beam, up to 150 μA @ 155 MeV
- ERL-operation (MAGIX experiment): unpolarized beam, up to 1 (10) mA @ 105 MeV

Fig. 3: Schematic layout of the MESA accelerator

3.1 Brief description of the MESA accelerator

MESA (Mainz Energy-recovering Superconducting Accelerator) will use a spin polarized photo source with currents up to 1 mA. The beam time structure will be 1.3 GHz c.w. (continuous wave) which minimizes the bunch charges and therefore the beam dynamical issues associated with the charge. Nevertheless, space charge related effects are still important. The P2 experiment requires sophisticated spin manipulation techniques which lead to a relatively long low energy beam transport system between the source and the injector linac. Therefore larger currents than 1 mA will be difficult to handle, hence for experiments with even higher demands, we plan to install another source for an unpolarized beam closer to the injector linear accelerator (ILAC), which will allow us to achieve 10 mA of beam current.

After passing the injector the beam will have 5 MeV and can be injected in the first cryomodule where an energy gain of 25 MeV is achieved by 2 slightly modified TESLA-type cavities. The beam is then sent through a spreader, a 180 degree deflection and a recombiner which latter is almost identical to the spreader, and then enters the second cryomodule. The different recirculation arcs can be used to pass the cryomodules 3 times, yielding 155 MeV for external beam operation with the P2 experiment. This experiment is not of direct relevance here since it operates with the conventionally extracted beam. The “MAGIX” (MAInz Internal Gas target Experiment) experiment is integrated in another recirculation loop where 105 MeV will be the beam energy. To operate the experiment, the recirculation loop is extended into an additional hall in which the beam passes the MAGIX target and is sent back to the main linac. Since the loop represents a net 180 degree phase shift the beam is decelerated again through 2 recirculations. Afterwards, the beam leaves at the opposite side with respect to the injection point at 5 MeV.

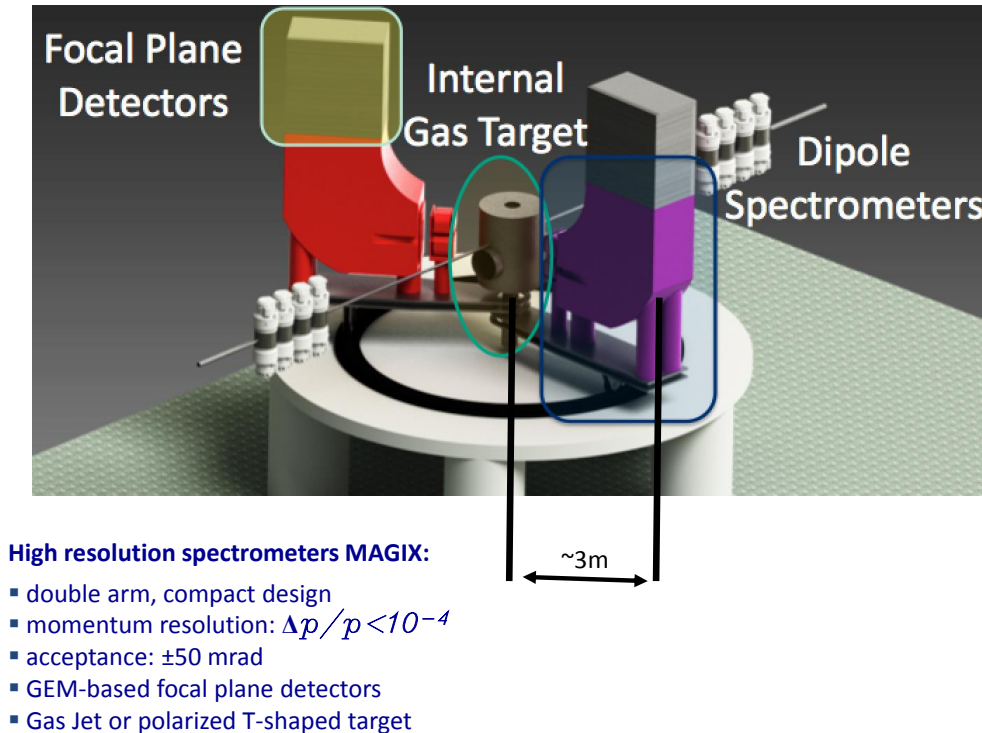


Fig. 4: Artists view of the MAGIX setup [13]

3.2 The MAGIX experiment

Figure 4 gives an impression of the planned MAGIX setup. Two magnetic spectrometers are employed in order to perform coincidence experiments. The spectrometers operate with a bending radius ≈ 1 m which indicates that the setup will be quite compact. They can achieve a momentum resolution of $\Delta p/p < 10^{-4}$. This sets a corresponding requirement for the energy definition of the MESA beam which should be at least the same or preferentially have a lower value. Specific detector systems are currently being designed which take into account the low energies of the scattered particles.

The target region is separated from the beam line vacuum by a differential pumping stage. Modern jet or cluster targets allow high areal densities $> 5 \times 10^{18} \text{cm}^{-2}$ (see Section 4.1 below). With the planned beam current of MESA stage-1 (1 mA) this results in a luminosity of $> 3 \times 10^{34} \text{s}^{-1} \text{cm}^{-2}$. Figure 5 shows the angular distribution after a beam with no angular spread has hit such a hydrogen target. The distribution has been produced by Monte Carlo simulation with Geant 4. The resulting widening of the angular distribution is negligible in terms of the natural divergence of an electron beam, at least as far as the root-mean-square value of the angular straggling is concerned.

However, this does not mean that operation of such a target with an ERL beam is straightforward. It is obvious that trajectories at arbitrary angles will exist due to elastic scattering. For very large angles ($\theta > 5$ deg) such particles may reach the detectors and can be considered as a signal. For small angles ($\theta < 10$ mrad) particles may fit into the acceptance of the beamline and the subsequent deceleration system. Particles in the interval between these regions are target-induced halo and must be absorbed (collimated) at well-defined positions. The stopping process should ideally not produce background in the detectors or produce radiation levels that could become harmful for hardware installed in the areas behind the target.

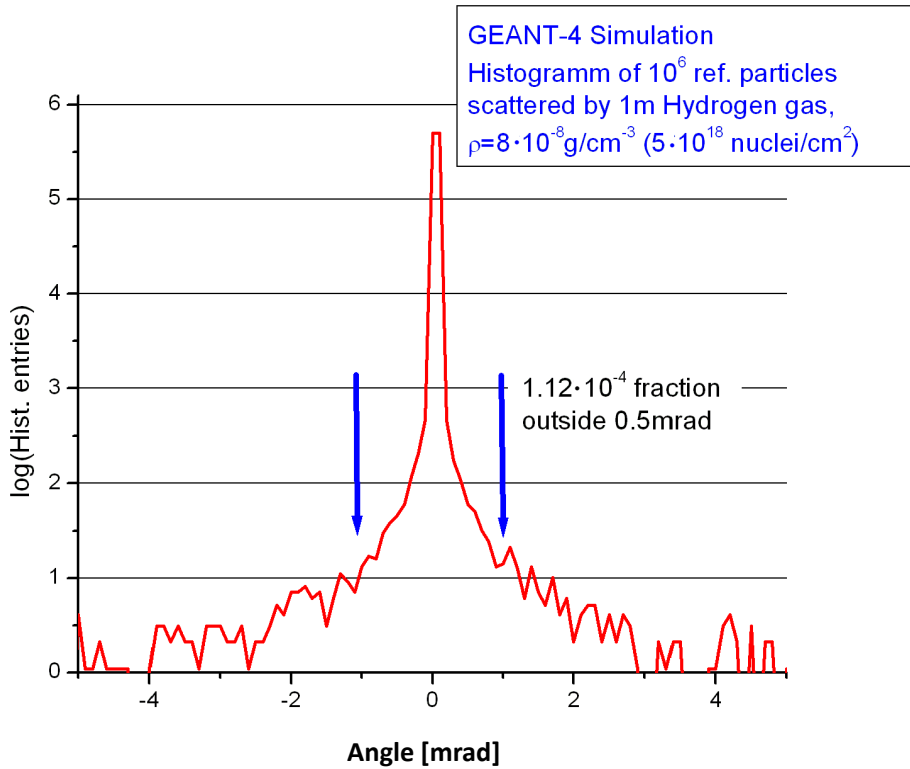


Fig. 5: Angular electron distribution behind target

3.3 Low background reactions: dark photons

The ‘dark photon’ (denoted here by γ') is a hypothetical gauge particle that could explain several anomalies related to astrophysical observations or the (g-2) anomaly of the muon [14]. Such a particle would behave like a photon but would have rest mass. The observations hint at a particle mass of the γ' of between 1 and 1000 MeV.

Since a gauge particle represents a force carrier, a charge is attributed to it. Though its effective interaction with ordinary matter will be very small, it is not zero. This is expressed via the Feynman graph in Fig. 6. In a scattering process radiation occurs, the vast majority of which is photon bremsstrahlung, but in very rare cases the dark photon could be produced due to the charge which causes a coupling ϵ .

If the dark photon preferentially decays into electron/positron pairs, the total energy of the pair will correspond to the rest mass of the γ' . Hence, if one observes such pairs and measures their momentum, a continuous background spectrum will be reconstructed on which the sharp peak resulting from the mass of the γ' is superimposed. The sensitivity of such a discovery increases with the resolution of the detectors, which motivates the use of magnetic spectrometers. Such measurements have been performed for instance at the Mainz Mikrotrotron (MAMI), but also at many other accelerators, although a γ' has so far not been discovered [15, 16].

These measurements allow us to exclude certain ranges of charge and mass for the dark photon. The current (2016) status of this exclusion is presented in Fig. 7. MAGIX can cover hitherto uncovered area in the parameter space for $2 \text{ MeV} \leq m_{\gamma'} < 80 \text{ MeV}$ and for couplings $10^{-3} \geq \epsilon > 5 \times 10^{-5}$. Besides this, there is an even more interesting argument to use MAGIX in a slightly modified way.

In a specific region of the parameter space (red hatched area in Fig. 7) the observed (g-2) anomaly

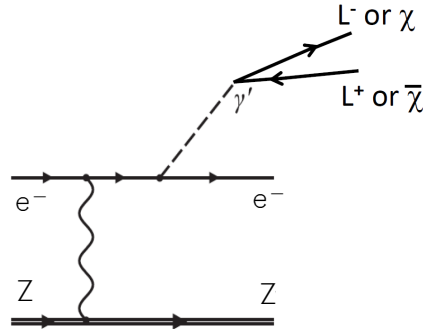


Fig. 6: Feynman graph for dark photon (γ') production during electromagnetic scattering on a nucleus of charge Z . The γ' could decay either into a lepton/antilepton pair (L^+/L^-) or into dark matter particles ($\chi/\bar{\chi}$).

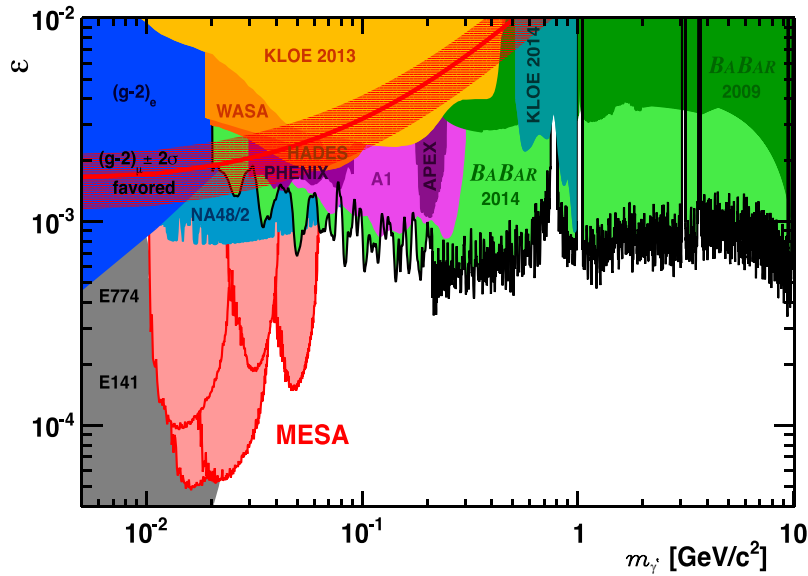


Fig. 7: Exclusion plots for the dark photon based on the assumption of a dominant reaction channel $\gamma' \rightarrow e^+ + e^-$

of the muon could be explained by the existence of a γ' , but it has not been discovered there. However, the exclusion limits have been achieved under the assumption that the decay into e^+/e^- -pairs is the dominant reaction channel. This may not be the case if dark particles $\chi, \bar{\chi}$ exist into which the γ' could decay preferentially (Fig. 6). In this case, a wide region of the interesting area remains unexplored. The χ - dark matter particles are invisible to detectors. Nevertheless, the rest mass of the γ' can still be reconstructed if the energy of the outgoing scattered electron and the recoil energy of the nucleus are measured. Due to the low recoil energy this is difficult in conventional targets but can be achieved in the windowless gas target of MAGIX.

3.4 Precision observables: form factors

Form factors are ground state properties of composite systems, for instance the proton. They depend on the four momentum transfer Q^2 in elastic scattering. Of particular interest is the extrapolation of the form factor towards $Q^2 = 0$. The slope of this extrapolation at $Q^2 = 0$ defines the charge radius of the particle. For the proton an exciting situation has occurred recently which has been dubbed the ‘proton

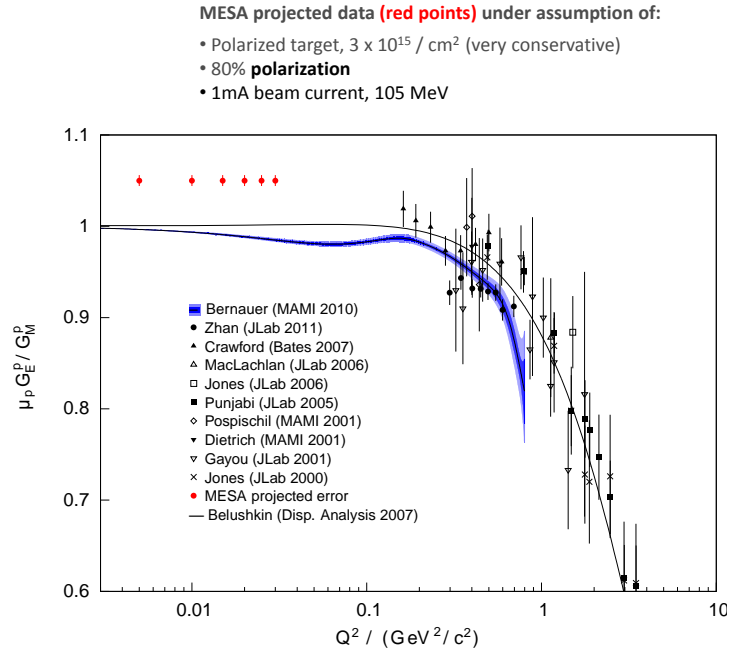


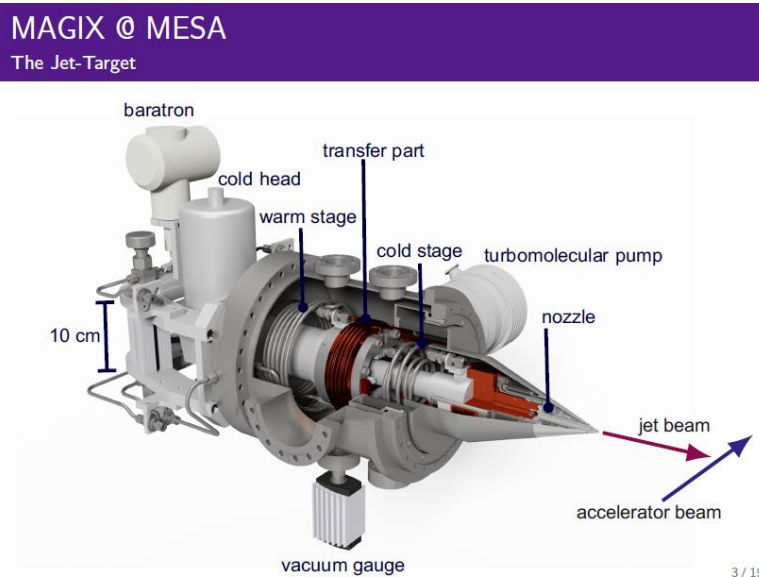
Fig. 8: Existing magnetic form factor data can be extended to much lower momentum transfers with the MAGIX setup using a 1 mA spin polarized beam. The red points stand for the expected accuracy of the data in the hitherto unexplored region of momentum transfers. The references given correspond to different experiments and extrapolations that were undertaken during the last two decades [18–27].

radius puzzle’. This has been caused by the availability of high precision spectroscopic data from muonic hydrogen atoms which do not agree with the data obtained by electron scattering [17, 18]. The situation calls for data at lower momentum transfer in the electron scattering experiments, which so far have not been achievable due to the aforementioned strong beam target interaction in conventional experiments. Figure 8 presents the situation for the ratio of the electric to the magnetic form factor. The theoretical extrapolation (solid line) can be checked by MAGIX data points at the indicated level of precision, if an intense spin polarized beam is available .

It should be mentioned that MAGIX can also be used to observe other ground state properties such as the electromagnetic polarizabilities of the nucleons. To summarize, it can be stated the outlook for a rich physics program in low energy hadron physics at MAGIX looks very promising.

3.5 Nuclear physics at MAGIX

The possibility of exploring low momentum transfers opens new windows also for nuclear physics. For instance, in nuclear astrophysics, the reaction $^{12}\text{C} + \alpha \rightarrow ^{16}\text{O} + \gamma$ is highly important for stellar evolution but is so far not accessible experimentally due to the low energies relevant here. This can be changed by using MAGIX if the inverse reaction $^{16}\text{O} + \gamma^* \rightarrow ^{12}\text{C} + \alpha$ is investigated. Here, electron scattering creates exchange of a virtual photon γ^* . Again, the extrapolation to the photon point (mass of exchanged particle = $Q^2 = 0$) will deliver the desired information.



S. Grieser ;<https://indico.mitp.uni-mainz.de/event/66/session/5/contribution/27/material/slides/0.pdf>

Fig. 9: The jet target foreseen for MAGIX at MESA

4 Instrumentation for ERLs operating for particle physics

4.1 Windowless targets

In Fig. 9 we present the target setup which is presently discussed for MESA. Present day designs allow for unpolarized densities of 10^{19} cm^{-2} for various gas species [28], whereas polarized gas targets are much more difficult to handle. They need the application of a storage cell—typically about one 0.3–1 m long with a small aperture to increase the gas density inside. Such targets can achieve only $\approx 10^{16} \text{ cm}^{-2}$ with high nuclear polarization. Experiments with such targets therefore require high electron currents, moreover, since single spin asymmetries are not particularly interesting in this energy range, a spin polarized electron beam is needed to perform double polarization experiments.

4.2 Spin polarized beams at ERLs

Spin polarized beams are produced by photoemission from so-called semiconductor superlattices [29]. Typically GaAs/GaAsP layers of a few nanometres thickness form a basic period which is repeated many times. This lifts the light hole/ heavy hole degeneracy in the semiconductor and allows therefore the efficient transfer of the angular momentum of the photons towards the spin of the electrons. In reality, this means that circularly polarized light can be transformed to spin polarized electrons inside the conduction (mini-) band of the superlattice. After photoexcitation, the electrons diffuse towards the surface from where they can escape if the work function of the photocathode is lowered by about a mono-atomic layer of caesium plus a certain amount of fluorine or Oxygen atoms [30]. The degree of spin polarization may reach almost 90% at typical laser wavelengths in the near infra-red (IR) (780 nm). The quantum efficiency at this wavelength can approach 1% which is in more practical units about 5 mA of electron current per watt of incident laser power. Modern laser systems can produce enough laser power to allow the production of a 100 mA electron beam which is presently a typical goal for light source ERLs [31] and spin polarized currents for the electron–ion collider projects are typically a little bit lower.

However, the weak point of the chain is the sustainability of the beam current, which is expressed by the so-called cathode lifetime τ . The lifetime during which the quantum efficiency drops to $1/e$ of its initial value is electron current dependent. This is due to the ionization of the residual gas which causes back bombardment of the cathode and corresponding radiation damage. The highest average currents that have been achieved for reasonable operation times (>100 hours) are a few milliamperes only. The product $I \cdot \tau$ is called the charge lifetime [32]. There are indications that it is not current, but the electron fluence, which limits the lifetime, i.e. the extracted charge per square centimetre. Since the beam emittance is proportional to the beam radius at the cathode, one cannot increase the extractable charge during one lifetime arbitrarily without increasing the beam emittance. However, for a large acceptance injector, which could accept a normalized emittance of $\approx 20 \mu\text{m}$ in theory, charge lifetimes of 10 000 coulombs or more can be expected which could make operation for a collider feasible. Nevertheless, there are remaining challenges here. They can for instance be addressed by further lowering the base pressure and in consequence the amount of ion back bombardment. This could, for instance, be achieved by a cryogenic system and there is hope that, for instance, higher lifetimes could be observed in superconducting Radio-Frequency (RF-)guns. Another approach is being pursued at BNL where the beam time structure of the proposed eRHIC collider makes it possible to funnel beams from several cathodes onto a common orbit by interleaving them with a time-dependent deflector. This scheme has been called the ‘Gatling-gun’ and is currently under development at BNL [33].

In summary, the problem of lifetime should be tractable at the level desired for the collider projects but the effort and the resources needed should not be underestimated.

Acknowledgements

I wish to thank the organizers of the CAS workshop for giving me the opportunity to present these contents. This work has been supported by the Deutsche Forschungsgemeinschaft DFG through the cluster of excellence PRISMA.

References

- [1] M. Tigner, *Nuovo Chim.* **37**(3) (1965) 1228. <https://doi.org/10.1007/BF02773204>
- [2] A. Jankowiak, these proceedings.
- [3] N. Berger *et al.*, *J. Univ. Sci. Tech. China* **46** (2016) 481.
- [4] S. Heinemeyer *et al.*, arXiv:0705.4056v2 (2007).
- [5] E. Steffens and W. Haeberli, *Rep. Prog. Phys.* **66**(11) (2003) 1887. <https://doi.org/10.1088/0034-4885/66/11/R02>
- [6] R. Alarcon *et al.*, *Phys. Rev. Lett.* **111**(16) (2013) 164801. <https://doi.org/10.1103/PhysRevLett.111.164801>
- [7] E. Metral (editor), ICFA Beam Dynamics Newsletter **58** (2012) 52.
- [8] E. Metral (editor), ICFA Beam Dynamics Newsletter **58** (2012) 86.
- [9] A. Assmann *et al.*, Energy calibration with resonant depolarization at LEP, Proceedings third European Accelerator Conference EPAC 1994, London 935-937 (1994)
- [10] B.S. Schlimme *et al.*, *Nucl. Instrum. Meth. A* **850** (2017) 54. <https://doi.org/10.1016/j.nima.2017.01.024>
- [11] Y.H. Wu *et al.*, Beam dynamics studies for coherent electron cooling experiment, Proceedings IPAC2016, WEPOY023 (2016), <http://accelconf.web.cern.ch/AccelConf/ipac2016/papers/wepmw027.pdf>.
- [12] A. Chao and M. Tigner (editors), *Handbook of Accelerator Physics and Engineering* (World Scientific, Singapore, 2002), p. 128.

- [13] A. Denig, Workshop New Vistas in Low Energy Particle Physics, Mainz, 2016, <https://indico.mitp.uni-mainz.de/event/66/overview>
- [14] G.W. Bennett *et al.*, *Phys. Rev. D* **73**(7) (2006) 072003. <https://doi.org/10.1103/PhysRevD.73.072003>
- [15] J.P. Lees *et al.*, BaBar Collaboration, *Phys. Rev. Lett.* **113**(20) (2014) 201801. <https://doi.org/10.1103/PhysRevLett.113.201801>
- [16] H. Merkel *et al.*, A1 Collaboration, *Phys. Rev. Lett.* **106**(25) (2011) 251802. <https://doi.org/10.1103/PhysRevLett.106.251802>
- [17] R. Pohl *et al.*, *Nature* **466**(7303) (2010) 213. <https://doi.org/10.1038/nature09250>
- [18] J.C. Bernauer *et al.*, *Phys. Rev. Lett.* **105**(24) (2010) 242001. <https://doi.org/10.1103/PhysRevLett.105.242001>
- [19] X. Zhan *et al.*, *Phys. Lett B* **705**(49) (2011). <https://doi.org/10.1016/j.physletb.2011.10.002>
- [20] J.B. Crawford *et al.*, *Phys. Rev. Lett.* **98** (2011) 052301. <https://doi.org/10.1103/PhysRevLett.98.052301>
- [21] G. MacLachlan *et al.*, *Nucl. Phys. A* **764** (261) (2006). <https://doi.org/10.1016/j.nuclphysa.2005.09.012>
- [22] M. K. Jones *et al.*, *Phys. Rev. C* **74** (2006) 242301. <https://doi.org/10.1103/PhysRevC.74.035201>
- [23] V. Punjabi *et al.*, *Phys. Rev. C* **71** (2005) 055202. <https://doi.org/10.1103/PhysRevC.71.055202>
- [24] T. Pospichil *et al.*, *Eur. Phys. J. A* **12** (125) (2001). <https://doi.org/10.1007/s100500170046>
- [25] O. Gayou *et al.*, *Phys Rev C* **64** (2001) 038202. <https://doi.org/10.1103/PhysRevC.64.038202>
- [26] M. K. Jones *et al.*, *Phys. Rev. Lett.* **84** (1398) (2000). <https://doi.org/10.1103/PhysRevLett.84.1398>
- [27] M. A. Belushkin *et al.*, *Phys. Rev. C* **75** (2007) <http://dx.doi.org/10.1103/PhysRevC.75.035202>
- [28] S. Grieser, Workshop New Vistas in Low Energy Particle Physics, Mainz, 2016, <https://indico.mitp.uni-mainz.de/event/66/overview>
- [29] T. Maruyama *et al.*, *Appl. Phys. Lett.* **85**(13) (2004) 2640. <https://doi.org/10.1063/1.1795358>
- [30] W.E. Spicer and A. Herrera-Gomez, Modern theory and applications of photocathodes, SLAC-PUB-6306, (1993), <http://slac.stanford.edu/pubs/slacpubs/6250/slac-pub-6306.pdf>
- [31] G.H. Hoffstatter, S.M. Gruner, M. Tigner (editors), Cornell Energy Recovery Linac, Project definition report (2013). <https://www.classe.cornell.edu/rsrc/Home/Research/ERL/ErlPubs2013/PDDR.pdf>
- [32] J. Grames *et al.*, Lifetimes Measurements of high polarization strained superlattice gallium arsenide at beam current > milliamp using a new 100 kV load lock photogun, Proceedings PAC2007, THPMS064 (2007). <http://accelconf.web.cern.ch/AccelConf/p07/PAPERS/THPMS064.PDF>
- [33] X. Chang *et al.*, A multiple cathode gun design for the eRHIC polarized electron source, Proceedings PAC 2011, WEP263 (2011) 1969. <http://accelconf.web.cern.ch/AccelConf/PAC2011/papers/wep263.pdf>